© 2018. Published by The Company of Biologists Ltd | Journal of Cell Science (2018) 131, jcs213884. doi:10.1242/jcs.213884

RESEARCH ARTICLE

# The Ajuba family protein Wtip regulates actomyosin contractility during vertebrate neural tube closure

**Chih-Wen Chu‡, Bo Xiang*,‡, Olga Ossipova, Andriani Ioannou and Sergei Y. Sokol§**

## ABSTRACT

Ajuba family proteins are implicated in the assembly of cell junctions and have been reported to antagonize Hippo signaling in response to cytoskeletal tension. To assess the role of these proteins in actomyosin contractility, we examined the localization and function of Wtip, a member of the Ajuba family, in *Xenopus* early embryos. Targeted *in vivo* depletion of Wtip inhibited apical constriction in neuroepithelial cells and elicited neural tube defects. Fluorescent protein-tagged Wtip showed predominant punctate localization along the cell junctions in the epidermis and a linear junctional pattern in the neuroectoderm. In cells undergoing Shroom3-induced apical constriction, the punctate distribution was reorganized into a linear pattern. Conversely, the linear junctional pattern of Wtip in neuroectoderm changed to a more punctate distribution in cells with reduced myosin II activity. The C-terminal fragment of Wtip physically associated with Shroom3 and interfered with Shroom3 activity and neural fold formation. We therefore propose that Wtip is a tension-sensitive cytoskeletal adaptor that regulates apical constriction during vertebrate neurulation.

This article has an associated First Person interview with the first author of the paper.

**KEY WORDS: Apical constriction, Junctions, Shroom3, *Xenopus*, Wilms tumor-1-interacting protein, Tension**

## INTRODUCTION

Ajuba LIM family members are ubiquitous LIM domain-containing proteins implicated in the regulation of cell junctions and signaling (Kadrmas and Beckerle, 2004; Schimizzi and Longmore, 2015). The N- and C-terminal domains of these proteins have been proposed to physically interact, although the evidence for this interaction has been largely indirect (Sun and Irvine, 2013). The single *Drosophila* gene homologue *Jub* regulates organ size in fly embryo development (Rauskolb et al., 2014). In vertebrates, *in vivo* functions of this family remain poorly characterized because of potential redundancy of the three closely related genes encoding Limd1, Ajuba and Wilms tumor-1-interacting protein (Wtip) (Schimizzi and Longmore, 2015).

Ajuba family proteins are present in multiple locations in the cell, possibly reflecting diverse molecular functions. *Drosophila* Jub is present at apical cell junctions in wing disc epithelial cells and this distribution depends on mechanical tension (Rauskolb et al., 2014; Sabino et al., 2011). Similarly, mammalian Ajuba localizes to adherens junctions and was shown to bind α-catenin, thereby linking adherens junctions and the actin cytoskeleton (Marie et al., 2003). At the junctions, Ajuba modulates Rac1 activity and inactivates Lats kinase to inhibit Hippo signaling (Das Thakur et al., 2010; Nola et al., 2011). Ajuba and Wtip were also found in the nucleus (Kanungo et al., 2000; Kim et al., 2010; Langer et al., 2008; Srichai et al., 2004), and Ajuba family proteins are known to interact with Snail2 transcriptional repressors to activate neural crest specific transcription (Langer et al., 2008). In addition, Ajuba family proteins were found at the centrosomes of mammalian cells and fly neuroblasts (Hirota et al., 2003; Sabino et al., 2011). This localization has been associated with the control of cell division, centrosome positioning and mitotic spindle orientation (Sabino et al., 2011; Schimizzi and Longmore, 2015). Moreover, Wtip has been implicated in planar polarity and ciliogenesis in *Xenopus* and zebrafish embryos (Bubenshchikova et al., 2012; Chu et al., 2016). Taken together, these observations highlight the roles of Ajuba family proteins as adaptors mediating signaling between different cell compartments.

To gain additional knowledge about this protein family, we examined the localization and functions of Wtip in *Xenopus* embryonic ectoderm. Gain- and loss-of-function studies of Wtip revealed its role as a mechanosensitive cytoskeletal adaptor required for apical constriction during vertebrate neural tube closure. The N- and C-terminal domains of Wtip exhibited different localization in ectoderm cells but colocalized when expressed together. Moreover, we observed that Wtip associates with the actin-binding protein Shroom3, a key player in apical constriction (Haigo et al., 2003; Hildebrand and Soriano, 1999), providing a potential mechanism for Wtip to modulate actomyosin contractility.

## RESULTS

### Wtip is required for apical constriction in the *Xenopus* neural plate

To interfere with the function of Wtip in developing *Xenopus* embryos, we used previously described antisense morpholino oligonucleotides (MOs) that efficiently block *Wtip* mRNA translation *in vivo* (Chu et al., 2016). Depletion of Wtip inhibited neural fold formation and resulted in neural tube defects (Fig. 1A-D). The defects were predominantly in the anterior portion of the neural tube, consistent with the notion that the neural tube 'zippers' in *Xenopus* embryos from the posterior towards the anterior aspect. The severity and frequency of these phenotypes were suppressed by *wtip* mRNA, confirming specificity. These defects were unlikely to be due to abnormal cell division, since the nuclear morphology appeared to be normal in *Wtip* morphants (Fig. S1A,B). Similar neural tube defects were observed in embryos injected with a second Wtip MO with a different sequence, but not in those injected with a control MO (Fig. 1D and data not shown). At later stages, neural tube deficiencies became less pronounced; however, mild axial and eye

Department of Cell, Developmental and Regenerative Biology, Icahn School of Medicine at Mount Sinai, New York, NY 10029, USA.
*Present address: Cancer Research Institute, Central South University, Changsha, Hunan 410078, China.
‡These authors contributed equally to this work

§Author for correspondence (sergei.sokol@mssm.edu)

S.Y.S., 0000-0002-3963-9202

**Received 7 December 2017; Accepted 6 April 2018**

Journal of Cell Science (2018) 131, jcs213884. doi:10.1242/jcs.213884

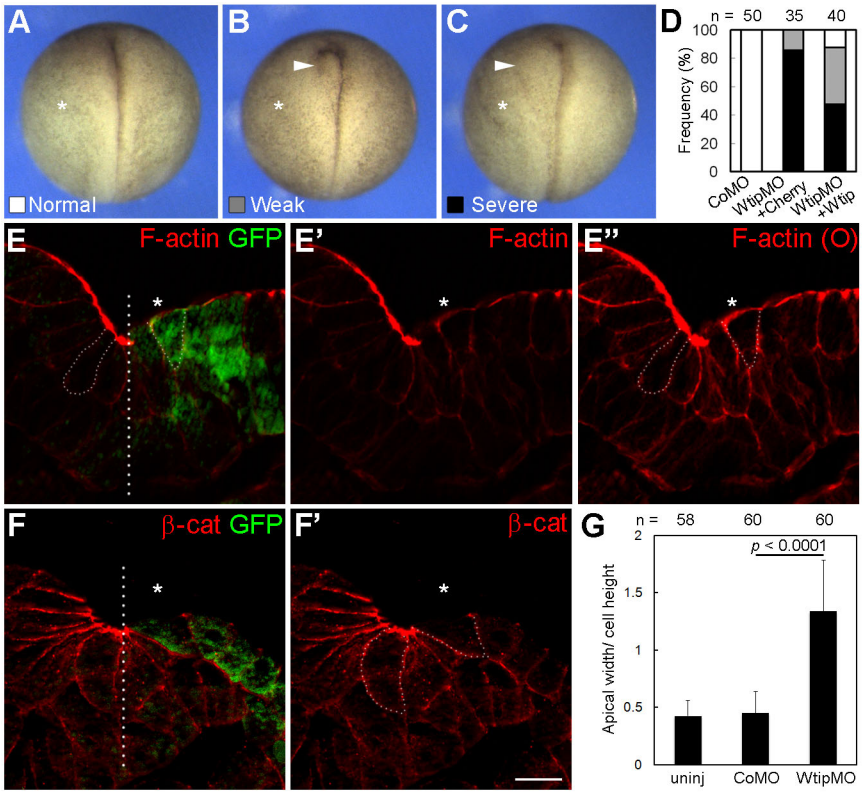


**Fig. 1. Wtip is required for neural tube closure.** (A-C) Embryos were unilaterally injected into presumptive ectoderm with control MO (CoMO), WtipMO1 (7.5 ng each) plus membrane-mCherry (Cherry, 75 pg) or HA-RFP-Wtip RNA (Wtip, 75 pg) and cultured until stage 19. Neural tube closure defects were categorized as 'normal', 'weak' or 'severe' as shown. Asterisks mark the injected side, and arrowheads indicate neural folds that fail to undergo apical constriction. (D) Frequencies of neural tube defects. Data are from three independent experiments. Two-tailed Fisher's exact test: Control MO to WtipMO1 +Cherry, $P<0.0001$; WtipMO1+Cherry to WtipMO1 +Wtip, $P=0.0011$. (E-F′) Four- to eight-cell embryos were unilaterally injected with WtipMO1 plus GFP RNA (100 pg) and fixed at stage 17. Representative cryosection of the neural ectoderm was stained for GFP and F-actin (E-E″) or β-catenin (β-cat, F,F′). Asterisks indicate the injected side. Cell borders visible after overexposure (O) are indicated by dashed lines to reveal cell shape. Compared with the uninjected side, Wtip-depleted superficial cells (marked by GFP) failed to constrict apically or accumulate apical F-actin. The midline is indicated, apical is up. Scale bar: 20 µm. (G) Apical constriction of medially positioned superficial cells quantified as the ratio of apical width to apicobasal height. Means±s.d. are shown. Uninj, uninjected side. *n*, number of cells scored. Statistical significance was determined by the Student's *t*-test. Data are from two independent experiments.

defects have been observed (Fig. S1C-E′). These observations suggest that Wtip functions in vertebrate neural tube closure.

Apical constriction in the *Xenopus* neural plate is visible by the formation of the dorsolateral hinges (Colas and Schoenwolf, 2001; Suzuki et al., 2012), which is suppressed in Wtip-depleted embryos (Fig. 1B,C, arrowheads). To examine whether this hinge formation defect is due to the failure of apical constriction, cryosections of embryos were stained with Phalloidin to visualize F-actin. F-actin was enriched at the apical surfaces of constricting neuroepithelial cells, as previously reported (Rolo et al., 2009), but this enrichment was not detected in cells containing Wtip MO and lineage tracer (Fig. 1E,E′). In addition, cells depleted of Wtip had wider apical surfaces compared with those in cells in the uninjected half of the neural plate (Fig. 1E-G). Together, these findings indicate that Wtip is required for apical constriction during vertebrate neurulation.

### Subcellular localization of Wtip and its fragments in embryonic ectoderm

To investigate the subcellular localization of Wtip in *Xenopus* ectoderm, fusions of Wtip with fluorescent proteins were constructed and expressed in early embryos. In superficial ectoderm cells during gastrulation, HA-RFP-Wtip was localized at the cellular junctions and in cytoplasmic puncta (Fig. 2A). At stage 12, the junctional puncta became more predominant in the epidermis (Fig. 2B). Frequently, the junctional puncta were visible in both neighboring cells as doublets positioned across the cell junctions (Fig. 2B′,C-C″). At stage 14, the cytoplasmic puncta of Wtip were more abundant (Fig. 2D-D″). In contrast, in neural ectoderm, Wtip showed continuous junctional staining and was enriched at the tricellular junctions, which was similar to the distribution of F-actin (Fig. 2E-E″). Tricellulin, a marker for tricellular junctions, was surrounded by Wtip (Fig. 2F-F″, arrows), implying the involvement of Wtip in tension sensing at the tricellular junction (Higashi and Miller, 2017). At later stages, Wtip was retained in cytoplasmic puncta and localized to the basal bodies of skin multiciliated cells (Fig. S2A). This is consistent with the reported centrosomal localization of Ajuba family proteins in several cell types (Chu et al., 2016; Hirota et al., 2003; Sabino et al., 2011). GFP-tagged Wtip exhibited a similar subcellular distribution (data not shown).

We next wanted to define specific protein sequences needed to localize Wtip to the puncta and the centrosome/basal body. Several truncated constructs were generated, including the N-terminal fragment (WtipN, amino acids 1-480) containing repeated serine-rich motifs and the C-terminal fragment (WtipC, amino acids 481-690) with three conserved LIM domains (Fig. 3A). As observed for full-length Wtip, WtipN also formed highly organized peri-junctional puncta visualized in both live embryos and fixed samples (Fig. 3B,B′ and data not shown). In contrast, WtipC was largely present at the cortex and in the nucleus (Fig. 3C,F), in agreement with the reported nuclear localization signal (Kanungo et al., 2000; Srichai et al., 2004). Of note, the small region between amino acids 1-250 was sufficient to target GFP to the centrosome and basal body, but not cortical puncta (Fig. S2B,C). These experiments reveal distinct targeting signals in Wtip.

The junctional punctate signal of Wtip and WtipN often appeared as a doublet across the cell border. Images of neighboring cells expressing either HA-RFP-WtipN or GFP-WtipN revealed pairing of differently colored puncta along the cell junction (Fig. 3D-D″), confirming that their positions are coordinated across the cell membrane. Since this pattern is reminiscent of sarcomere-like actomyosin complexes observed in some epithelial cells (Choi et al., 2016; Ebrahim et al., 2013; Fanning et al., 2012), we examined colocalization of Wtip with several actin- and myosin-interacting proteins. We found that the distribution of Moesin actin-binding domain (Moe-GFP), a marker of F-actin (Edwards et al., 1997; Skoglund et al., 2008), occasionally alternated with the position of

Journal of Cell Science (2018) 131, jcs213884. doi:10.1242/jcs.213884

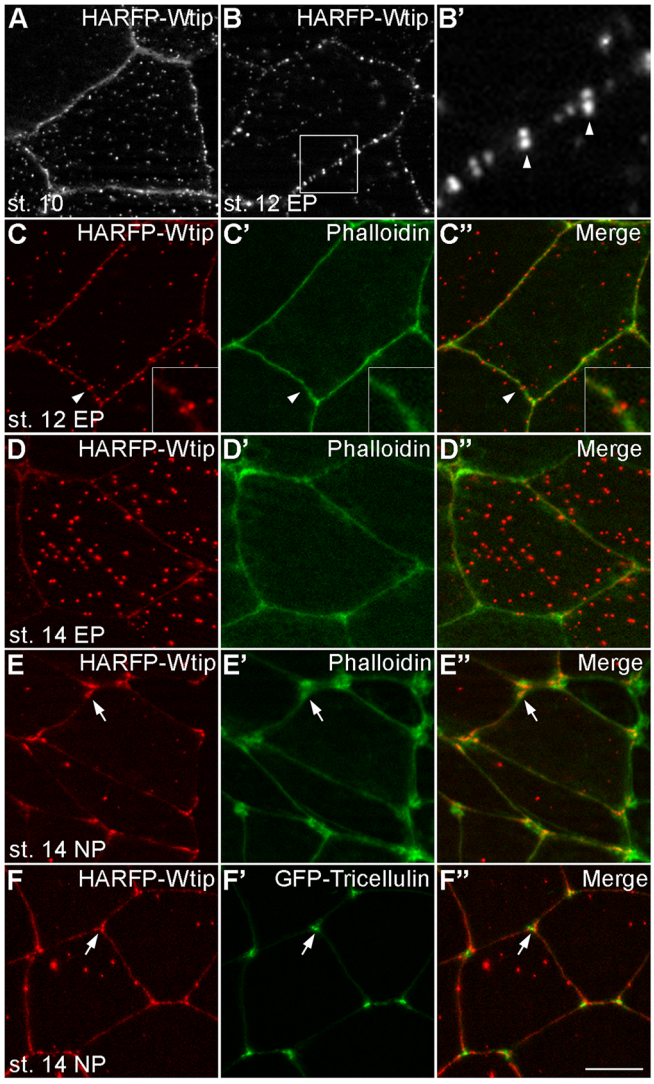


**Fig. 2. Dynamic subcellular localization of Wtip in *Xenopus* embryonic ectoderm.** HA-RFP-Wtip RNA (200 pg) was injected into animal blastomeres of *Xenopus* four-cell embryos. The injected embryos were fixed at different stages and superficial ectoderm was imaged. (A) Stage 10 gastrula ectoderm; (B,B′) stage 12 epidermal ectoderm. The boxed area in B is enlarged in B′. Note the punctate distribution of Wtip along the cell junctions, with some puncta paired across the junction (arrowheads). (C-E″) Stage 12 (C-C″) or stage 14 (D-D″) epidermal ectoderm or stage 14 neuroectoderm (E-E″) stained with Phalloidin to visualize F-actin at the cell junctions. Arrowheads indicate a pair of Wtip puncta on the opposite sides of the junction, which is enlarged in the inset. Note the presence of Wtip at tricellular junctions (arrows). (F-F″) Stage 14 neuroectoderm coinjected with HA-RFP-Wtip and GFP-Tricellulin (50 pg) RNAs. The Wtip signal surrounds Tricellulin at tricellular junctions (arrows). Scale bar: 10 µm. Representative images from three to five independent experiments are shown, and each group included explants from 8-12 embryos.

WtipN puncta (Fig. 3E-E″). However, Phalloidin or α-actinin staining did not exhibit a punctate pattern (Fig. 2C′ and data not shown), suggesting that a specific yet uncharacterized pool of F-actin may play a role in the regulation of Wtip localization.

### Interaction of the N- and C-terminal Wtip domains

Zyxin is a LIM-domain protein that is closely related to the Ajuba family. Previous studies support a model in which Zyxin maintains a ‘closed’ conformation as a result of the intramolecular interaction between its N- and C-terminal domains (Hirota et al., 2000;

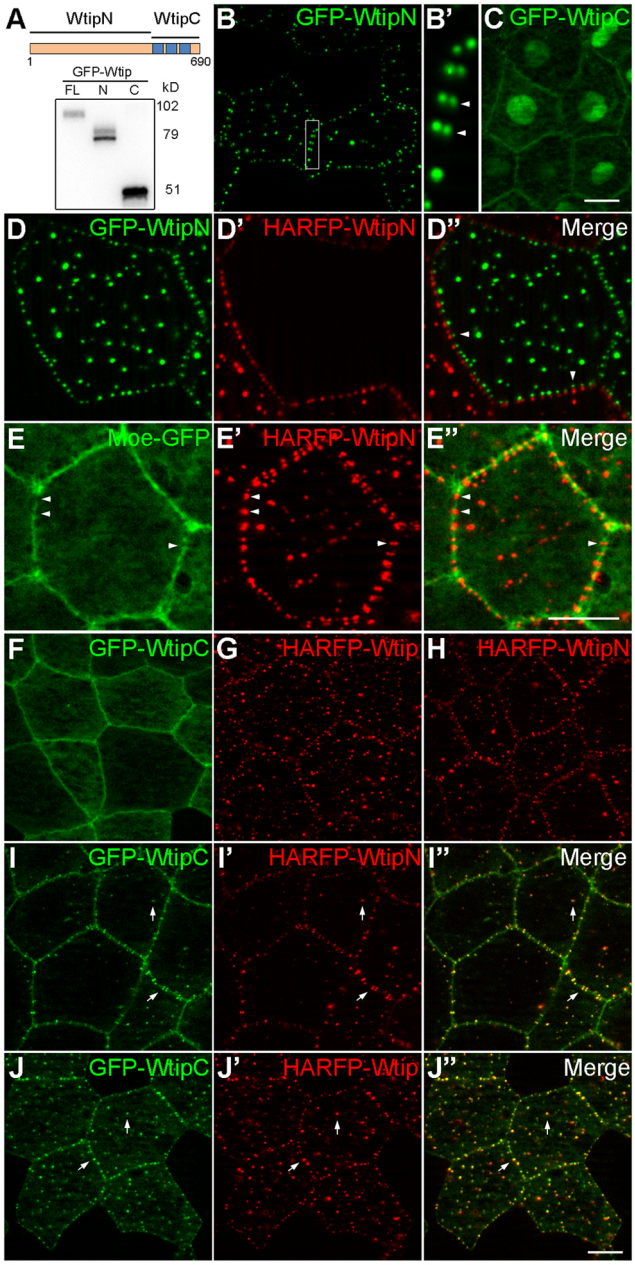


**Fig. 3. Interaction of the N- and C-terminal domains of Wtip in the epidermal ectoderm.** (A) Scheme (top) and protein expression levels of Wtip constructs. Anti-GFP immunoblot analysis of gastrula lysates expressing GFP-Wtip fusions [left to right: full length Wtip (FL), WtipN (N), WtipC(C)]. Approximate molecular sizes are indicated. (B-C,F-J″) Embryos were injected ventroanimally with 300 pg of indicated RNAs and imaged at stage 12. (B,B′,C) Live images of embryos expressing GFP-WtipN (B,B′) or GFP-WtipC (C). The boxed area in B is enlarged in B′. Note WtipN puncta paired across the junction in adjacent ectodermal cells (arrowheads in B′). (D-D″) GFP-WtipN and HA-RFP-WtipN RNA (300 pg each) were injected into two adjacent ventral blastomeres, respectively, and embryos showing mosaic expression pattern were fixed and imaged at stage 12. Note the red and green puncta paired across the cell boundary (arrowheads). (E-E″) RNAs encoding HA-RFP-WtipN (300 pg) and Moe-GFP (250 pg) were injected animally into the ventral blastomere, and epifluorescence at stage 12 is shown. Gaps in Moe-GFP distribution that correspond to WtipN enrichment sites are indicated by arrowheads. (F-J″) Apical images of fixed epidermal ectoderm expressing indicated Wtip constructs alone (F-H) or in combination with WtipC (I-J″). Note the colocalization of WtipC with Wtip or WtipN in cortical puncta upon coexpression (arrows). Scale bars: 10 µm. Representative images from four independent experiments are shown, and each group included explants from 8-12 embryos.

Journal of Cell Science (2018) 131, jcs213884. doi:10.1242/jcs.213884

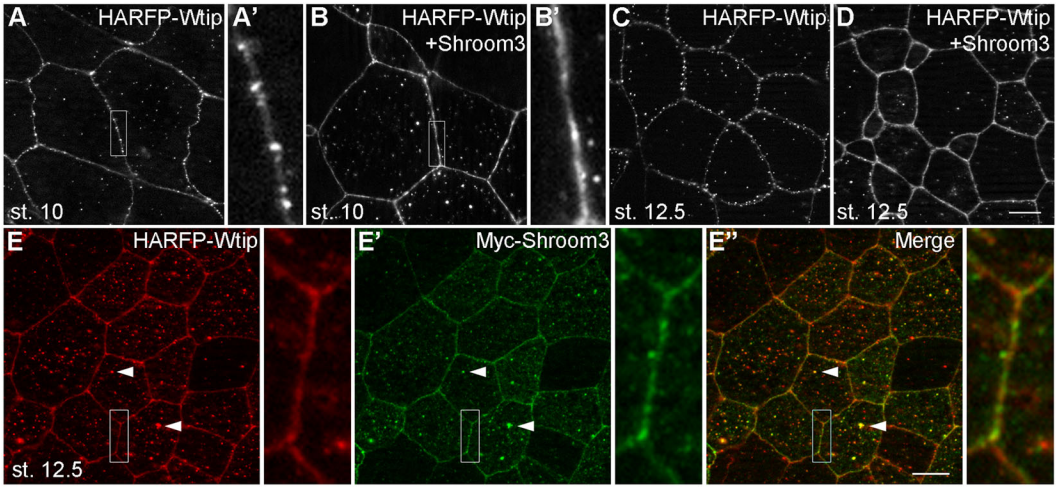


**Fig. 4. Regulation of Wtip localization by apical constriction.** Embryos injected with HA-RFP-Wtip (200 pg) with or without Myc-Shroom3 (125 pg) RNA were fixed at indicated stage. The apical side of the epidermal ectoderm was imaged. Representative images from four independent experiments are shown, and each group contained explants from 8-12 embryos. (A,A′,C) Punctate distribution of Wtip along the junction. (B,B′,D) Continuous distribution of Wtip along the junction in response to Shroom3. The boxed areas in A and B are enlarged in A′ and B′, respectively. (E-E″) Shroom3 localization is visualized by staining for Myc (green). Note the colocalization of Wtip and Shroom3 at the junctions (boxed area, enlarged on the right) and cortical puncta (arrowheads). Scale bars, 10 µm.

Moody et al., 2009). We therefore examined whether a similar interaction exists in Wtip by coexpressing WtipC with WtipN or full-length Wtip. WtipC was recruited to the cortical puncta containing full-length Wtip or WtipN (Fig. 3F-J″), providing evidence for association of the two domains *in vivo*.

### Wtip junctional localization is altered in a tension-dependent manner

Because apical constriction is known to generate actomyosin-dependent tension (Martin and Goldstein, 2014), we examined whether Wtip distribution is modulated by Shroom3, which induces ectopic apical constriction in *Xenopus* ectoderm (Haigo et al., 2003) by recruiting Rho-associated kinase to apical junctions (Das et al., 2014; Nishimura and Takeichi, 2008). In ectodermal cells overexpressing Shroom3, the punctate localization of HA-RFP-Wtip at the junctions was rearranged into a continuous pattern (Fig. 4A-D). This change was visible at the onset of apical constriction (Fig. 4A-B′) and became more evident over time (Fig. 4C,D). HA-RFP-Wtip was partially colocalized with Shroom3 at the junctions and cytoplasmic puncta (Fig. 4E-E″). This finding suggests that Wtip is recruited to apical junctional complexes in response to increased cytoskeletal tension.

Since Wtip is redistributed to junctional complexes in response to enhanced actomyosin contractions, we wanted to test its localization in cells with reduced myosin activity. This complementary experiment was carried out in the neuroectoderm, in which Wtip localization at cell junctions is continuous (Fig. 2E,F). Myosin function is inhibited by Mypt1T696A, a constitutively active form of the myosin light chain phosphatase subunit Mypt1 (Weiser et al., 2009). Upon coexpression of Mypt1T696A, Wtip distribution became more punctate, both in the cytoplasm and at the junctions, and the enrichment of Wtip at the tricellular junctions was diminished (Fig. 5A,B). Unlike full-length Wtip, neither WtipN nor WtipC revealed any sensitivity to Mypt1T696A (Fig. 5C-F). Our observations therefore suggest that Wtip responds to mechanical tension triggered by actomyosin contractions and that both the N- and C-terminal domains are required for this process.

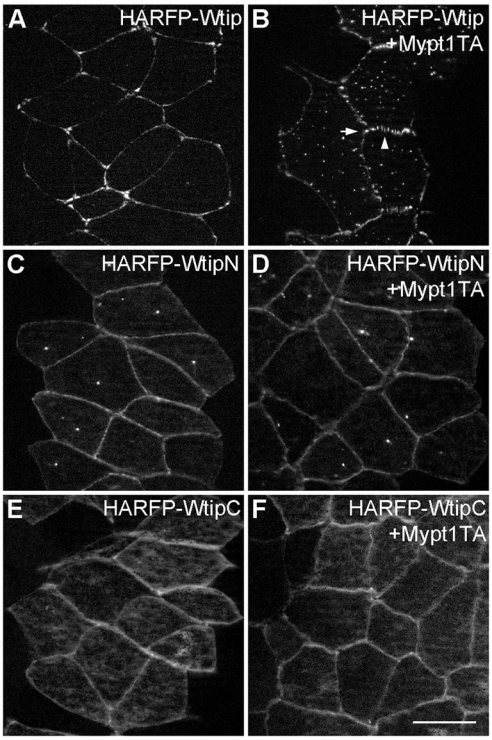


**Fig. 5. Regulation of Wtip localization by myosin II phosphatase.** *En face* view of fixed stage 15 neural plate explants from embryos injected with indicated HA-RFP-Wtip RNAs (200 pg each) with (B,D,F) or without (A,C,E) Mypt1T696A (Mypt1TA, 100 pg) RNAs. Note the loss of Wtip enrichment at the tricellular junction (arrow) and punctate Wtip signals along the junction (arrowhead) in response to Mypt1T696A (B). Representative images from two independent experiments are shown, and each group included explants from 8-12 embryos. Scale bar: 20 µm.

Journal of Cell Science (2018) 131, jcs213884. doi:10.1242/jcs.213884

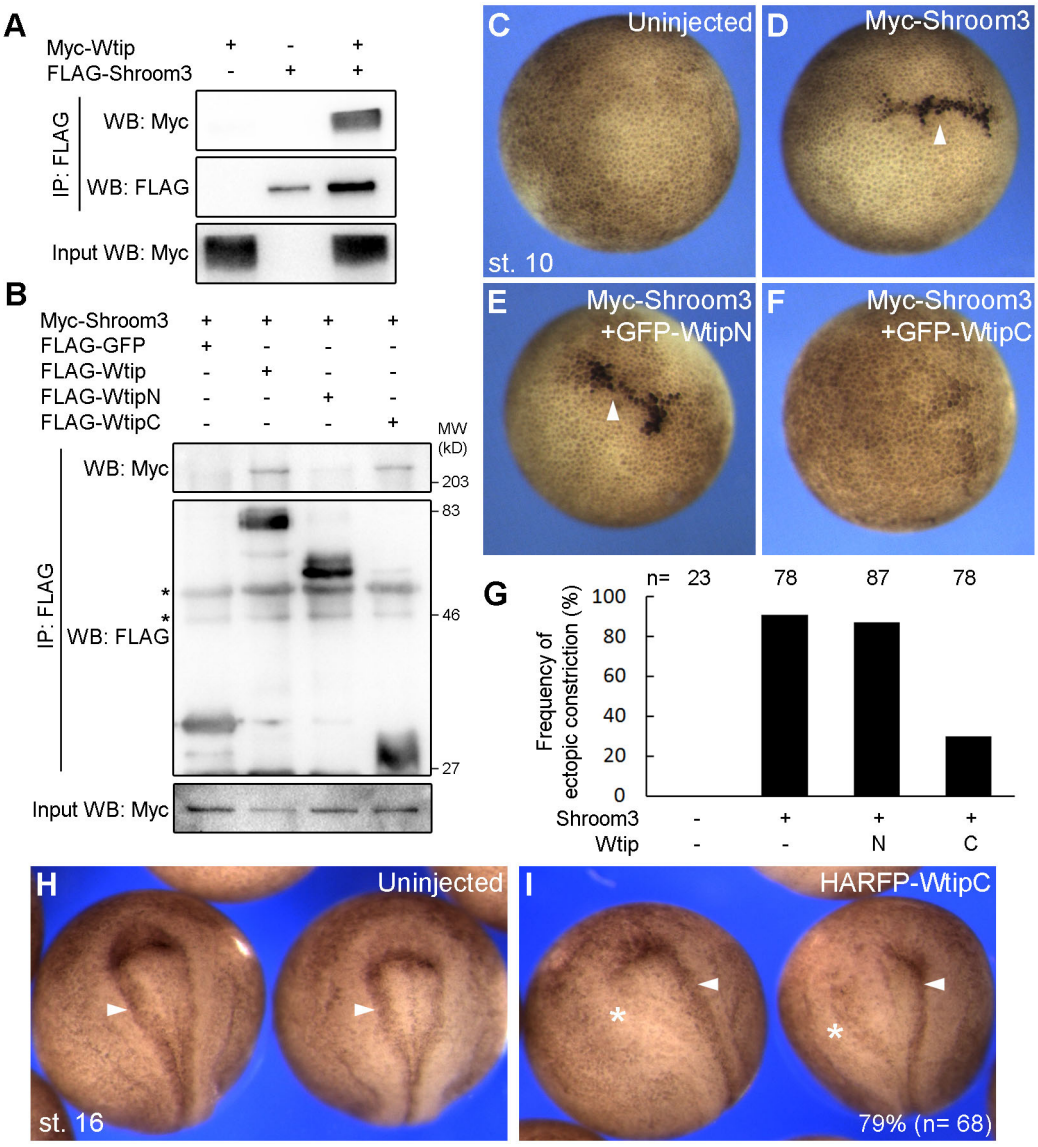


**Fig. 6. Wtip associates with Shroom3 and modulates apical constriction.** (A) HEK293T cells were transfected with Flag-Shroom3 and Myc-Wtip DNAs. Immunoprecipitation with anti-FLAG agarose shows specific co-precipitation of Wtip and Shroom3. (B) Embryos injected with indicated RNAs were lysed at stage 12 and subjected to immunoprecipitation. Shroom3 is pulled down by Wtip or WtipC, but not by WtipN. Asterisks mark nonspecific signals. (C-G) Effects of Wtip constructs on Shroom3 activity. Embryos were injected with indicated RNAs and cultured until stage 10 for imaging. (C) Uninjected control embryo. (D) Myc-Shroom3 RNA (100 pg) induced ectopic apical constriction accompanied by hyper-pigmentation of ectoderm cells (arrowheads). This phenotype was suppressed by RNA encoding GFP-WtipC (F) but not GFP-WtipN (E) (1 ng each) in five independent experiments. (G) Frequencies of embryos with ectopic apical constriction are shown. Total number of embryos scored is indicated above each bar. (H,I) Embryos unilaterally injected with HA-RFP-WtipC (2 ng) were imaged at stage 16. WtipC inhibited the formation of the hinge lines at the injected side (asterisks) compared with the control side or uninjected embryos (arrowheads). Frequencies of the phenotype (%) and the numbers of scored embryos are shown.

### The interaction of WtipC and Shroom3 modulates apical constriction

Since both Shroom3 and Wtip are junctional, and Shroom3 affects Wtip localization, we tested whether Wtip physically interacts with Shroom3. Immunoprecipitation analysis using transfected HEK293T cells revealed the binding of Shroom3 to Wtip (Fig. 6A). This binding was confirmed by a reciprocal pull-down experiment using mRNA-injected embryos, and we further demonstrated that Shroom3 binds specifically to WtipC rather than WtipN (Fig. 6B). When coexpressed with Shroom3 in the ectoderm, WtipC, but not WtipN, blocked Shroom3-mediated apical constriction almost completely (Fig. 6C-G). Moreover, overexpression of WtipC on one side of the embryo caused a unilateral neural tube defect (Fig. 6H,I), which was similar to the defect in Wtip-depleted embryos (Fig. 1A-D). Taken together, these observations suggest that Wtip regulates neural tube closure by modulating Shroom3-dependent apical constriction via its C-terminus.

We next examined whether Wtip constructs can modulate the localization of Myc-Shroom3. At the onset of apical constriction, Shroom3 showed punctate distribution at the cell junctions and cytoplasm, and this pattern remained unchanged upon WtipN expression (Fig. 7A,B). However, in cells overexpressing WtipC, staining of Shroom3 was reduced at the junctions and became more diffuse in the cytoplasm (Fig. 7C). The protein level of Shroom3 was not affected by the expression of WtipN or WtipC (Fig. 7D).

Journal of Cell Science (2018) 131, jcs213884. doi:10.1242/jcs.213884

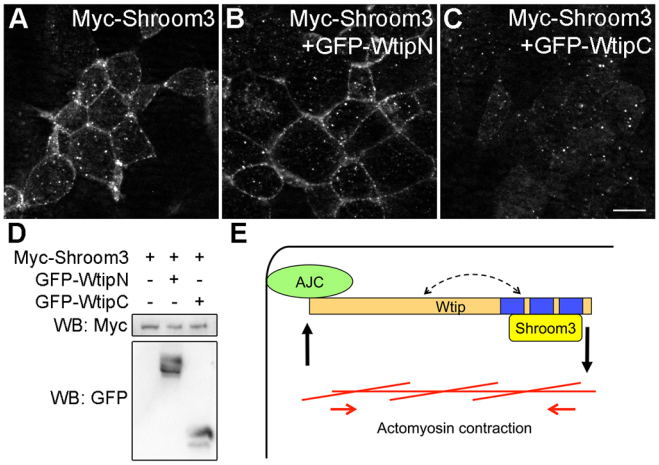


**Fig. 7. WtipC interferes with Shroom3 localization at the junctions.** Embryos were injected with indicated RNAs as described in the legend of Fig. 6D-F. (A-C) Stage 10 gastrula ectoderm was stained with anti-Myc antibody. Note the lack of junctional staining in cells expressing GFP-WtipC (C). Scale bar: 10 µm. The images are representative of three different experiments. (D) Protein expression was analyzed by western blot. Shroom3 expression level is not affected by WtipN or WtipC. (E) A positive feedback model for apical constriction. Wtip associates with the apical junctional complex (AJC) via its N-terminus, whereas its C-terminal domain binds to and recruits Shroom3 to the apical junctions. The increased tension during apical constriction promotes further recruitment of Wtip to the AJC. Wtip function may also be regulated by an intramolecular interaction between its N- and C-terminus (dashed arrow).

These experiments suggest that WtipC blocks Shroom3-induced apical constriction by displacing Shroom3 from the cell junctions.

We also tested whether binding of Wtip to Shroom3 is sensitive to tension. Mypt1T696A was co-expressed with Wtip and Shroom3 to reduce tension, and its effect was visualized by the reduction of apical constriction in all injected embryos (Fig. S3A). Immunoprecipitation analysis showed that similar amounts of Shroom3 were pulled down by Wtip regardless of the presence of Mypt1T696A (Fig. S3B), suggesting that binding of Wtip to Shroom3 is not regulated by a change in tension.

## DISCUSSION

This study evaluated the functions of *Xenopus* Wtip, an Ajuba family protein, in embryonic ectoderm. Previous studies implicated Wtip in neural crest specification and ciliogenesis in *Xenopus* embryos (Chu et al., 2016; Langer et al., 2008) and, *in vitro*, in the adhesion of mouse podocytes (Kim et al., 2012). Our depletion and interference experiments suggest that an important developmental function of Wtip is to mediate apical constriction during neural tube closure. We propose that Wtip is a cytoskeletal adaptor that regulates actomyosin contractility at the apical junctions. This novel function of Wtip expands the list of the cellular and developmental processes that involve the Ajuba family.

Mechanical forces generated by actomyosin contractions can alter protein conformation, binding partners and signaling activity, as has been demonstrated for the binding of vinculin to α-catenin (Yonemura et al., 2010). Consistent with this notion, Wtip puncta at the junctions are converted into a linear (continuous) distribution in response to apical constriction triggered by Shroom3. Moreover, relaxation of tension by Mypt1, which inhibits myosin II activity, leads to a complementary result: Wtip distribution is changed from a linear to a punctate pattern. We speculate that these localization patterns reflect the formation of diverse Wtip-containing protein complexes that are rearranged in a tension-dependent manner, which is somewhat similar to the behavior of Jub in *Drosophila* wing discs (Rauskolb et al., 2014). Interestingly, Wtip is localized at the tricellular junctions in a similar manner to vinculin (Higashi and Miller, 2017), implying a connection between Wtip and the vinculin–α-catenin complex under high tension. Notably, Ajuba can be recruited to adherens junctions through an interaction with α-catenin (Marie et al., 2003; Rauskolb et al., 2014), suggesting that Wtip might also associate with α-catenin. Future studies are required to address this possibility.

Since neither WtipN nor WtipC respond to Mypt1 in the neural plate, as full-length Wtip does, both domains are likely to contribute to Wtip function at the junctions. While the interacting partners of WtipN at the apical junctions remain unknown, we identified an association of WtipC with Shroom3. Given that it is still unclear how Shroom3 becomes localized to apical junctions (Hildebrand, 2005; Lang et al., 2014), we propose that Wtip functions as an adaptor that recruits Shroom3 to apical junctions to allow spatially restricted actomyosin contractions. The contraction increases junctional tension and, in turn, positively regulates Wtip localization to the junctions (Fig. 7E). Consistent with this model, overexpression of WtipC reduced Shroom3 junctional localization, inhibited Shroom3-mediated apical constriction and caused neural tube closure defects. However, Wtip MO caused only a slight change in Shroom3 localization (data not shown), possibly due to insufficient depletion or the presence of other Ajuba family proteins in this tissue. Alternatively, because Wtip localization changes in response to Shroom3, Shroom3 may function upstream of Wtip. At present, potential redundancies and feedback regulation at the apical junctions leave open the question of the epistatic relationship between Wtip and Shroom3.

Our experiments also revealed the interaction between the N- and C-terminal domains of Wtip. Upon coexpression, the puncta containing WtipN or Wtip also contained WtipC, consistent with an intramolecular or intermolecular interaction, in which the C-terminus of one Wtip molecule associates with the N-terminus of another, leading to head-to-tail aggregation. Notably, in Zyxin, this association has been proposed to lead to a ‘closed’ (i.e. inactive) conformation that prevents it from binding to phosphorylated VASP (Hirota et al., 2000; Moody et al., 2009). We found that Wtip and WtipC can pull down similar amounts of Shroom3, suggesting that binding of Shroom3 to WtipC is not blocked by WtipN. Future work will define the role of the WtipN-WtipC interaction in Wtip functions and evaluate whether it is regulated by mechanical forces and/or JNK-dependent phosphorylation, as proposed by recent studies (Rauskolb et al., 2014; Sun and Irvine, 2013).

## MATERIALS AND METHODS

### Plasmids, *in vitro* mRNA synthesis and morpholino oligonucleotides (MOs)

pCS2-Myc-Wtip (*Xenopus*) was a gift from Greg Longmore and Kris Kroll (Langer et al., 2008). The following plasmids have been previously described: pCS2-Myc-Shroom3 and pCS2-FLAG-Shroom3 (Chu et al., 2013; Plageman et al., 2010), pCS107-Moesin-GFP (Skoglund et al., 2008), pCS2-GFP-Tricellulin (Higashi et al., 2016), Mypt1T696A (Weiser et al., 2009), Histone-GFP (Petridou and Skourides, 2014). pCS2-GFP-Wtip and pCS105-HA-RFP-Wtip have been described (Chu et al., 2016). pCS2-GFP-WtipN and pCS105-HA-RFP-WtipN encodes amino acids 1-480 of Wtip. pXT7-GFP-WtipN251 encodes the first 251 amino acids of Wtip. pCS2-HA-RFP-WtipC and pCS2-GFP-WtipC encodes amino acids 481-690 of Wtip. Coding sequences of Wtip full-length, WtipN, and WtipC were subcloned into pCS2-FLAG. Details of plasmid construction are available upon request. Capped mRNAs were synthesized using

mMessage mMachine kits (Ambion, Austin, TX), according to manufacturer's instructions. MOs were purchased from Gene Tools (Philomath, OR, USA). The following MOs were used: control MO, 5′-GCTTCAGCTAGTGACACATGCAT-3′ (Ossipova et al., 2015), WtipMO1, 5′-TGTCCTCATCGTACTTCTCCATGTC-3′ (Chu et al., 2016).

### *Xenopus* embryo culture and microinjections

*In vitro* fertilization and culture of *Xenopus laevis* embryos were carried out as previously described (Dollar et al., 2005). The study was carried out in strict accordance with the recommendations in the Guide for the Care and Use of Laboratory Animals of the National Institutes of Health. The protocol 04-1295 was approved by the IACUC of the Icahn School of Medicine at Mount Sinai. Staging was according to Nieuwkoop and Faber (1994). For microinjections, four-cell embryos were transferred into 3% Ficoll in 0.5× MMR buffer (50 mM NaCl, 1 mM KCl, 1 mM $CaCl_2$, 0.5 mM $MgCl_2$, 2.5 mM HEPES pH 7.4) and 10 nl mRNA or MO solution was injected into one or more blastomeres. Amounts of injected mRNA per embryo have been optimized in preliminary dose-response experiments (data not shown).

### Sectioning, immunofluorescence staining and imaging

Ectodermal and neural plate explants were isolated from embryos fixed in MEMFA (0.1 M MOPS, pH 7.4, 2 mM EGTA, 1 mM $MgSO_4$ and 3.7% formaldehyde) (Harland, 1991). For sectioning, embryos fixed in MEMFA (for Phalloidin staining) or Dent's fixative (80% methanol+20% DMSO, for β-catenin staining) were embedded and cryosectioned using a Leica cryostat CM3050 at 10 µm as described previously (Ossipova et al., 2014). Indirect immunofluorescence staining was performed as described (Ossipova et al., 2014), the blocking solution was PBS+0.1% Triton X-100+3% BSA+3% goat serum. Mouse anti-GFP (B-2, Santa Cruz), rabbit anti-β-catenin (c2206, Sigma) and mouse anti-Myc (9E10 hybridoma) antibodies were used at 1:200, and Alexa Fluor 488-conjugated goat anti-mouse antibody (Invitrogen) and Cy3-conjugated donkey anti-mouse antibody (Jackson ImmunoResearch Laboratories) were used at 1:400. Alexa Fluor 488- or 568-conjugated Phalloidin (Thermo Fisher) were used for F-actin staining. Explants were mounted for observation in the Vectashield mounting medium (Vector Laboratories). Images were captured using a Zeiss AxioImager microscope with the Apotome attachment. AxioVision software (Zeiss) was used for image processing and measurements. Quantification of apical constriction was carried out using images of β-catenin-stained sections from 12 embryos. Apical width was defined as the distance between apical junctions, and cell height was defined as the distance between the midpoints of the apical and basal domains (Chu et al., 2013). Up to five superficial neuroectodermal cells adjacent to the midline were measured. Results shown are representative images from 2-4 independent experiments with 8-12 embryos per group.

### Cell culture and transfection

Human embryonic kidney 293T cells (ATCC) were maintained in DMEM (Corning) with 10% FBS (Gemini) and penicillin-streptomycin (Sigma). Cells growing at 70% confluence were transiently transfected using linear polyethylenimine (MW 25,000, Polysciences) as described (Ossipova et al., 2009). Each 35 mm dish of cells received 1.5 µg of pCS2 plasmids encoding FLAG-Shroom3 or Myc-Wtip as indicated. pCS2 vector DNA was added to plasmid DNA mixture to reach a total DNA amount of 3 µg.

### Immunoprecipitation and western blot analysis

For immunoprecipitation, cells transfected for 24 h were lysed in immunoprecipitation buffer (10 mM HEPES, pH 7.4, 150 mM NaCl, 1 mM EGTA, 1 mM $MgCl_2$, 1% Triton X-100, 1 mM $Na_3VO_4$, 10 mM NaF, 25 mM β-glycerol phosphate), containing protease inhibitor cocktail (cOmplete Mini EDTA-free, Roche). For *Xenopus* gastrula embryos, 50 mM NaCl was used instead of 150 mM to remove the majority of yolk proteins. After centrifugation at 15,000 ***g***, the supernatant was incubated with anti-FLAG agarose beads (Sigma) at room temperature for 2-3 h. The beads were washed, boiled in SDS-PAGE sample buffer, and subjected to SDS-PAGE and immunoblotting, essentially as described (Chu et al., 2013). The following primary antibodies were used: mouse anti-GFP (B-2, Santa Cruz), mouse anti-FLAG (M2, Sigma), mouse anti-Myc (9E10). Chemiluminescence was captured by the ChemiDoc MP imager (Bio-Rad).

#### Acknowledgements

We thank Ann Miller, Paul Skoglund, Ray Keller, Kristen Kroll and Greg Longmore for plasmids. We thank members of the Sokol laboratory for discussions.

#### Competing interests

The authors declare no competing or financial interests.

#### Author contributions

Conceptualization: C.-W.C., B.X, S.Y.S.; Methodology: C.-W.C., B.X., O.O., A.I., S.Y.S.; Validation: A.I.; Formal analysis: B.X., O.O., A.I.; Investigation: C.-W.C., B.X., O.O., A.I., S.Y.S.; Writing - original draft: C.-W.C., S.Y.S.; Writing - review & editing: C.-W.C., B.X., O.O., S.Y.S.; Visualization: C.-W.C., O.O.; Supervision: S.Y.S.; Funding acquisition: S.Y.S.

#### Funding

This study was supported by the National Institutes of Health (GM122492 to S.Y.S.). Deposited in PMC for release after 12 months.

#### Supplementary information

Supplementary information available online at
http://jcs.biologists.org/lookup/doi/10.1242/jcs.213884.supplemental

#### References

**Bubenshchikova, E., Ichimura, K., Fukuyo, Y., Powell, R., Hsu, C., Morrical, S. O., Sedor, J. R., Sakai, T. and Obara, T.** (2012). Wtip and Vangl2 are required for mitotic spindle orientation and cloaca morphogenesis. *Biol. Open* **1**, 588-596.

**Choi, W., Acharya, B. R., Peyret, G., Fardin, M.-A., Mège, R.-M., Ladoux, B., Yap, A. S., Fanning, A. S. and Peifer, M.** (2016). Remodeling the zonula adherens in response to tension and the role of afadin in this response. *J. Cell Biol.* **213**, 243-260.

**Chu, C.-W., Gerstenzang, E., Ossipova, O. and Sokol, S. Y.** (2013). Lulu regulates Shroom-induced apical constriction during neural tube closure. *PLoS ONE* **8**, e81854.

**Chu, C.-W., Ossipova, O., Ioannou, A. and Sokol, S. Y.** (2016). Prickle3 synergizes with Wtip to regulate basal body organization and cilia growth. *Sci. Rep.* **6**, 24104.

**Colas, J.-F. and Schoenwolf, G. C.** (2001). Towards a cellular and molecular understanding of neurulation. *Dev. Dyn.* **221**, 117-145.

**Das, D., Zalewski, J. K., Mohan, S., Plageman, T. F., VanDemark, A. P. and Hildebrand, J. D.** (2014). The interaction between Shroom3 and Rho-kinase is required for neural tube morphogenesis in mice. *Biol Open* **3**, 850-860.

**Das Thakur, M., Feng, Y., Jagannathan, R., Seppa, M. J., Skeath, J. B. and Longmore, G. D.** (2010). Ajuba LIM proteins are negative regulators of the Hippo signaling pathway. *Curr. Biol.* **20**, 657-662.

**Dollar, G. L., Weber, U., Mlodzik, M. and Sokol, S. Y.** (2005). Regulation of Lethal giant larvae by Dishevelled. *Nature* **437**, 1376-1380.

**Ebrahim, S., Fujita, T., Millis, B. A., Kozin, E., Ma, X., Kawamoto, S., Baird, M. A., Davidson, M., Yonemura, S., Hisa, Y. et al.** (2013). NMII forms a contractile transcellular sarcomeric network to regulate apical cell junctions and tissue geometry. *Curr. Biol.* **23**, 731-736.

**Edwards, K. A., Demsky, M., Montague, R. A., Weymouth, N. and Kiehart, D. P.** (1997). GFP-moesin illuminates actin cytoskeleton dynamics in living tissue and demonstrates cell shape changes during morphogenesis in Drosophila. *Dev. Biol.* **191**, 103-117.

**Fanning, A. S., Van Itallie, C. M. and Anderson, J. M.** (2012). Zonula occludens-1 and -2 regulate apical cell structure and the zonula adherens cytoskeleton in polarized epithelia. *Mol. Biol. Cell* **23**, 577-590.

**Haigo, S. L., Hildebrand, J. D., Harland, R. M. and Wallingford, J. B.** (2003). Shroom induces apical constriction and is required for hingepoint formation during neural tube closure. *Curr. Biol.* **13**, 2125-2137.

**Harland, R. M.** (1991). In situ hybridization: an improved whole-mount method for Xenopus embryos. *Methods Cell Biol.* **36**, 685-695.

**Higashi, T. and Miller, A. L.** (2017). Tricellular junctions: how to build junctions at the TRICkiest points of epithelial cells. *Mol. Biol. Cell* **28**, 2023-2034.

**Higashi, T., Arnold, T. R., Stephenson, R. E., Dinshaw, K. M. and Miller, A. L.** (2016). Maintenance of the epithelial barrier and remodeling of cell-cell junctions during cytokinesis. *Curr. Biol.* **26**, 1829-1842.

**Hildebrand, J. D.** (2005). Shroom regulates epithelial cell shape via the apical positioning of an actomyosin network. *J. Cell Sci.* **118**, 5191-5203.

**Hildebrand, J. D. and Soriano, P.** (1999). Shroom, a PDZ domain-containing actin-binding protein, is required for neural tube morphogenesis in mice. *Cell* **99**, 485-497.

**Hirota, T., Morisaki, T., Nishiyama, Y., Marumoto, T., Tada, K., Hara, T., Masuko, N., Inagaki, M., Hatakeyama, K. and Saya, H.** (2000). Zyxin, a regulator of actin filament assembly, targets the mitotic apparatus by interacting with h-warts/LATS1 tumor suppressor. *J. Cell Biol.* **149**, 1073-1086.

**Hirota, T., Kunitoku, N., Sasayama, T., Marumoto, T., Zhang, D., Nitta, M., Hatakeyama, K. and Saya, H.** (2003). Aurora-A and an interacting activator, the LIM protein Ajuba, are required for mitotic commitment in human cells. *Cell* **114**, 585-598.

**Kadrmas, J. L. and Beckerle, M. C.** (2004). The LIM domain: from the cytoskeleton to the nucleus. *Nat. Rev. Mol. Cell Biol.* **5**, 920-931.

**Kanungo, J., Pratt, S. J., Marie, H. and Longmore, G. D.** (2000). Ajuba, a cytosolic LIM protein, shuttles into the nucleus and affects embryonal cell proliferation and fate decisions. *Mol. Biol. Cell* **11**, 3299-3313.

**Kim, J. H., Konieczkowski, M., Mukherjee, A., Schechtman, S., Khan, S., Schelling, J. R., Ross, M. D., Bruggeman, L. A. and Sedor, J. R.** (2010). Podocyte injury induces nuclear translocation of WTIP via microtubule-dependent transport. *J. Biol. Chem.* **285**, 9995-10004.

**Kim, J. H., Mukherjee, A., Madhavan, S. M., Konieczkowski, M. and Sedor, J. R.** (2012). WT1-interacting protein (Wtip) regulates podocyte phenotype by cell-cell and cell-matrix contact reorganization. *Am. J. Physiol. Renal. Physiol.* **302**, F103-F115.

**Lang, R. A., Herman, K., Reynolds, A. B., Hildebrand, J. D. and Plageman, T. F. Jr.** (2014). p120-catenin-dependent junctional recruitment of Shroom3 is required for apical constriction during lens pit morphogenesis. *Development* **141**, 3177-3187.

**Langer, E. M., Feng, Y., Zhaoyuan, H., Rauscher, F. J., III, Kroll, K. L. and Longmore, G. D.** (2008). Ajuba LIM proteins are snail/slug corepressors required for neural crest development in Xenopus. *Dev. Cell* **14**, 424-436.

**Marie, H., Pratt, S. J., Betson, M., Epple, H., Kittler, J. T., Meek, L., Moss, S. J., Troyanovsky, S., Attwell, D., Longmore, G. D. et al.** (2003). The LIM protein Ajuba is recruited to cadherin-dependent cell junctions through an association with alpha-catenin. *J. Biol. Chem.* **278**, 1220-1228.

**Martin, A. C. and Goldstein, B.** (2014). Apical constriction: themes and variations on a cellular mechanism driving morphogenesis. *Development* **141**, 1987-1998.

**Moody, J. D., Grange, J., Ascione, M. P. A., Boothe, D., Bushnell, E. and Hansen, M. D. H.** (2009). A zyxin head-tail interaction regulates zyxin-VASP complex formation. *Biochem. Biophys. Res. Commun.* **378**, 625-628.

**Nieuwkoop, P. D. and Faber, J.** (1994). *Normal Table of Xenopus laevis (Daudin): A Systematical and Chronological Survey of the Development from the Fertilized Egg till the End of Metamorphosis*. New York: Garland Pub.

**Nishimura, T. and Takeichi, M.** (2008). Shroom3-mediated recruitment of Rho kinases to the apical cell junctions regulates epithelial and neuroepithelial planar remodeling. *Development* **135**, 1493-1502.

**Nola, S., Daigaku, R., Smolarczyk, K., Carstens, M., Martin-Martin, B., Longmore, G., Bailly, M. and Braga, V. M. M.** (2011). Ajuba is required for Rac activation and maintenance of E-cadherin adhesion. *J. Cell Biol.* **195**, 855-871.

**Ossipova, O., Ezan, J. and Sokol, S. Y.** (2009). PAR-1 phosphorylates Mind bomb to promote vertebrate neurogenesis. *Dev. Cell* **17**, 222-233.

**Ossipova, O., Kim, K., Lake, B. B., Itoh, K., Ioannou, A. and Sokol, S. Y.** (2014). Role of Rab11 in planar cell polarity and apical constriction during vertebrate neural tube closure. *Nat. Commun.* **5**, 3734.

**Ossipova, O., Chu, C.-W., Fillatre, J., Brott, B. K., Itoh, K. and Sokol, S. Y.** (2015). The involvement of PCP proteins in radial cell intercalations during Xenopus embryonic development. *Dev. Biol.* **408**, 316-327.

**Petridou, N. I. and Skourides, P. A.** (2014). FAK transduces extracellular forces that orient the mitotic spindle and control tissue morphogenesis. *Nat. Commun.* **5**, 5240.

**Plageman, T. F., Jr, Chung, M.-I., Lou, M., Smith, A. N., Hildebrand, J. D., Wallingford, J. B. and Lang, R. A.** (2010). Pax6-dependent Shroom3 expression regulates apical constriction during lens placode invagination. *Development* **137**, 405-415.

**Rauskolb, C., Sun, S., Sun, G., Pan, Y. and Irvine, K. D.** (2014). Cytoskeletal tension inhibits Hippo signaling through an Ajuba-Warts complex. *Cell* **158**, 143-156.

**Rolo, A., Skoglund, P. and Keller, R.** (2009). Morphogenetic movements driving neural tube closure in Xenopus require myosin IIB. *Dev. Biol.* **327**, 327-338.

**Sabino, D., Brown, N. H. and Basto, R.** (2011). Drosophila Ajuba is not an Aurora-A activator but is required to maintain Aurora-A at the centrosome. *J. Cell Sci.* **124**, 1156-1166.

**Schimizzi, G. V. and Longmore, G. D.** (2015). Ajuba proteins. *Curr. Biol.* **25**, R445-R446.

**Skoglund, P., Rolo, A., Chen, X., Gumbiner, B. M. and Keller, R.** (2008). Convergence and extension at gastrulation require a myosin IIB-dependent cortical actin network. *Development* **135**, 2435-2444.

**Srichai, M. B., Konieczkowski, M., Padiyar, A., Konieczkowski, D. J., Mukherjee, A., Hayden, P. S., Kamat, S., El-Meanawy, M. A., Khan, S., Mundel, P. et al.** (2004). A WT1 co-regulator controls podocyte phenotype by shuttling between adhesion structures and nucleus. *J. Biol. Chem.* **279**, 14398-14408.

**Sun, G. and Irvine, K. D.** (2013). Ajuba family proteins link JNK to Hippo signaling. *Sci. Signal.* **6**, ra81.

**Suzuki, M., Morita, H. and Ueno, N.** (2012). Molecular mechanisms of cell shape changes that contribute to vertebrate neural tube closure. *Dev. Growth Differ.* **54**, 266-276.

**Weiser, D. C., Row, R. H. and Kimelman, D.** (2009). Rho-regulated myosin phosphatase establishes the level of protrusive activity required for cell movements during zebrafish gastrulation. *Development* **136**, 2375-2384.

**Yonemura, S., Wada, Y., Watanabe, T., Nagafuchi, A. and Shibata, M.** (2010). alpha-Catenin as a tension transducer that induces adherens junction development. *Nat. Cell Biol.* **12**, 533-542.

## Supplementary figures

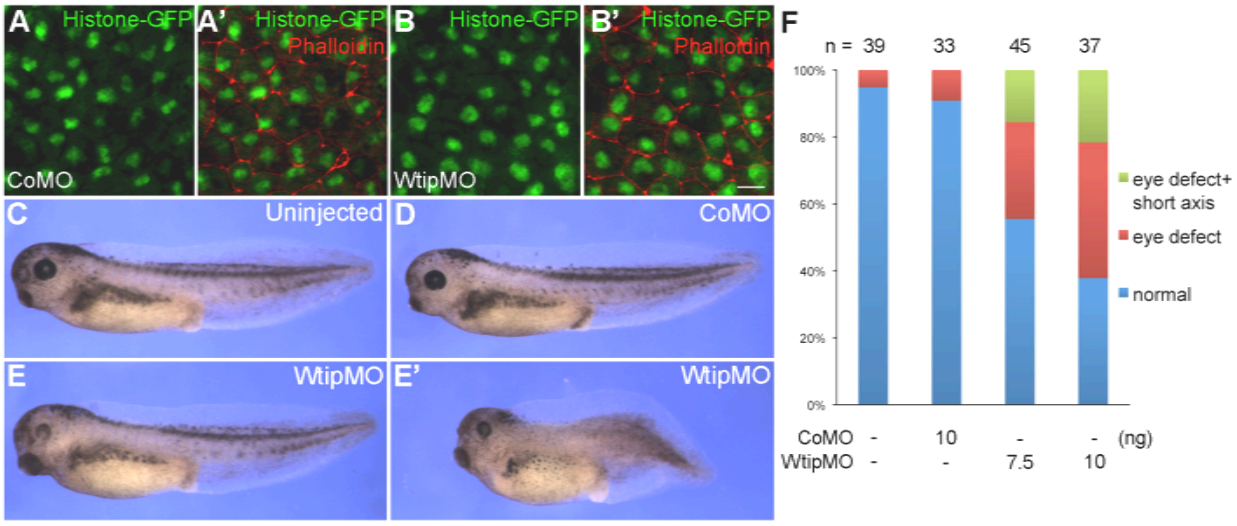


**Fig. S1. Phenotypes of WtipMO-injected embryos.**

RNAs encoding Histone-GFP (100 pg) and 7.5 ng of control (CoMO) or Wtip MO (WtipMO) were injected animally into one dorsal blastomere. (A-B') stage 10 animal caps stained with phalloidin to visualize cell boundaries. (C-F) stage 40 embryos uninjected or injected with indicated MOs. WtipMO caused eye defects and in some cases short body axis (E-E'). (F) Frequencies of the defects in the injected embryos. n, number of embryos per group. Data are collected from two independent experiments.

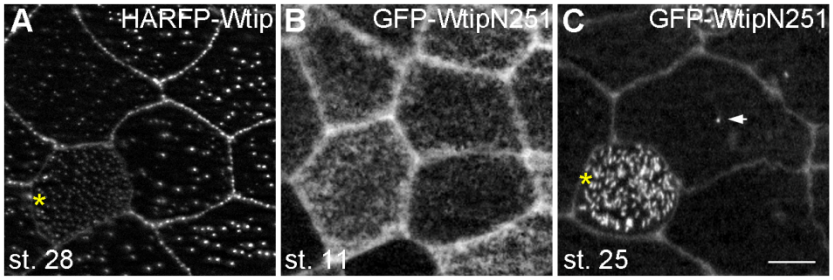


**Figure S2. Wtip is localized to the centrosomes and basal bodies.**

Embryos were injected with indicated RNA, and epifluorescence of epidermal ectoderm is shown at indicated stage. (A) At stage 28, HARFP-Wtip is detected at cell junctions, cytoplasmic puncta in goblet cells and basal bodies of multiciliated cells (asterisk). (B-C) Localization of GFP-WtipN251 at indicated stages. Note the strong signal at the cell junctions, centrosomes (arrow) and basal bodies (asterisk). Scale bar, 10 μm.

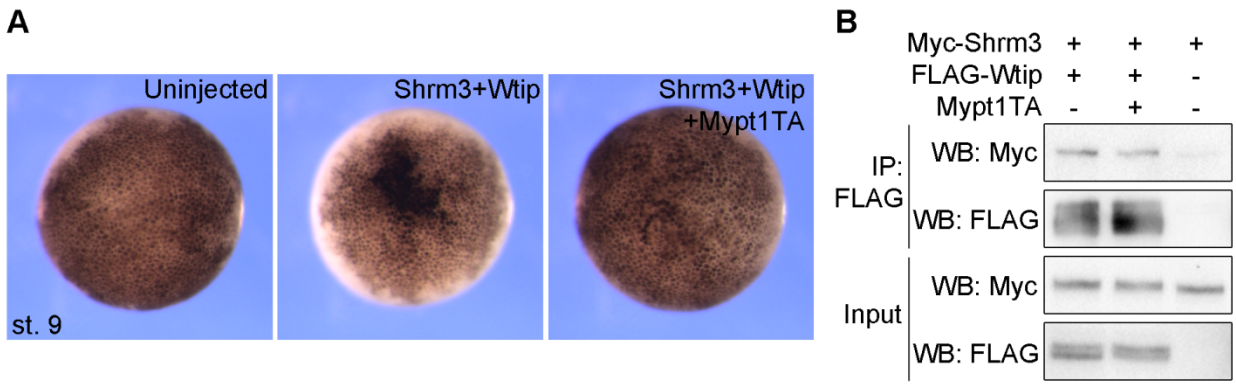


**Figure S3. The association between Wtip and Shroom3 is not regulated by tension.**
RNA injections and immunoprecipitation were carried out as described in Fig. 6 legend, with the addition of Mypt1T696A RNA (Mypt1TA, 100 pg). (A) Stage 9 embryos uninjected or injected with indicated RNAs. Note that Mypt1TA blocked Shroom3 (Shrm3)-induced cell pigmentation associated with apical constriction. (B) Embryos were lysed at stage 12 and subjected to immunoprecipitation. Similar amounts of Myc-Shroom3 were pulled down by FLAG-Wtip in the presence or absence of Mypt1TA.